Cytometry 6:238–253 (1985)

# Flow Cytometric Analysis of Mouse Spermatogenic Function Following Exposure to Ethylnitrosourea[1]

**Donald P. Evenson, Paul J. Higgins, Dorre Grueneberg, and Brenda E. Ballachey**

Department of Chemistry, South Dakota State University, Brookings, South Dakota (D.P.E., B.E.B.) and Laboratory of Investigative Cytology, Sloan-Kettering Research Institute, New York, New York (D.P.E., P.J.H., D.G.)

Received for publication May 3, 1984; accepted December 12, 1984

**The effects of the mutagenic agent ethylnitrosourea (ENU) on spermatogenic function and sperm chromatin structure were studied by flow cytometry and the results compared with sperm head morphology measurements. Groups of mice received daily exposures ranging from 0 to 75 mg/kg body weight × 5 days and were sacrificed 28 days later. Fresh testicular cell suspensions and epididymal sperm were stained with acridine orange (AO) and measured by flow cytometry. Sperm nuclei were isolated, fixed, rehydrated, and then either subjected to thermal stress or not prior to staining with AO. Body weights were unaffected by the chemical exposure while the testicular weights were reduced by about 50%. Two-parameter (DNA, RNA) flow cytometry measurements showed a dose-response relationship in the loss of certain cell types, particularly the elongated spermatids, from the testes of treated animals. Flow cytometric analysis of both heat-stressed and non-heat-stressed nuclei showed a relationship between dosage and the coefficient of variation of $\alpha_t$ {red/(red + green fluorescence)} measurements of AO stained nuclei, thereby demonstrating that alterations of chromatin structure occurred in response to ENU. Enzymatic digestions with RNAse, DNAse, and nuclease $S_1$ suggest that the increase in red fluorescence is due to an increase of single-stranded DNA induced by heat or acid treatment of chemically altered chromatin structure. The lowest daily dosage used (5 mg/kg) caused no significant changes in ratios of testicular cell types, a questionable increase in abnormal sperm head morphology and a detectable change in chromatin structure expressed as $\alpha_t$. This report shows that our technique for assaying sperm nuclear chromatin structure appears to have the same level of sensitivity to ENU induced nuclear alterations as the sperm head morphology test.**

**Key terms: Flow cytometry, sperm head morphology, toxicology, testis, chromatin structure**

The production of sperm represents one of the most dramatic examples of cellular proliferation and differentiation in any mammalian organ system. Although many biological parameters have been related to male fertility, sperm morphology is frequently used to assay testicular function. Sperm head morphology, consistent with nuclear morphology, is genotype specific (28), and is directed by genes on both the autosomes and sex chromosomes (2,41). Heritable changes in sperm head morphology can be induced by radiation and alkylating agents and followed quantitatively through successive generations (22,38,40).

Wyrobek and Bruce (42,43) developed a mouse model assay system to study the mutagenic and/or carcinogenic potential of chemicals using sperm head morphology as an end point. This test is relatively rapid and is considered very useful in the assessment of potentially toxic chemicals, since 100% of known mutagens tested were correctly identified as positives (44). Thus, demonstration of elevated levels of sperm abnormalities following exposure to a physical or chemical agent raises the possibility that the agent is inducing mutations in the germ cells (33,39).

Recently, we have developed a flow cytometric (FCM) assay of sperm chromatin structure (8) to determine the

Address reprint requests to Donald P. Evenson, Department of Chemistry, Box 2170, Animal Science Complex, South Dakota State University, Brookings, SD 57007.

[1]Supported by EPA grants No. R810986 and CR 810991 and NIH grant No. RO1 ES03035.

inherent stability of sperm nuclear DNA to thermal denaturation in situ and have found this assay to be useful in measuring effects of disease, diet, chemotherapy, and other factors on sperm nuclear chromatin structure (7,10,12). The work reported here on effects of ethylnitrosourea (ENU) and other ongoing research efforts (11) are testing the hypothesis that flow cytometric analysis of sperm samples from mice exposed to mutagenic and carcinogenic chemicals by the same protocol of Wyrobek and Bruce can rapidly detect chemically induced sperm defects and provide additional information not available by the sperm morphology test. Our two-parameter flow cytometric analysis for ratios of testicular cell types (14) present after chemical exposure is much more rapid than screening histology sections by light microscopy and provides more information than the one parameter FCM analysis more commonly used (33).

## MATERIALS AND METHODS

### Animal Care and Chemical Exposure

Five- to eight-week-old $F_1$ male mice (C57BL/6J female × C3H/HeJ male) were obtained from the Jackson Laboratory (Bar Harbor, ME) and kept for about 5 weeks prior to chemical exposure. These mice, having an average body weight of about 25 gm, were randomly separated into five groups of seven per group. The mice were housed in plastic cages with wire mesh tops and allowed free access to Purina Certified Rodent Laboratory Chow (No. 5002) and deionized water. Room temperature was maintained at 21 ± 2°C; lighting was on a 0700- to 1900-h schedule. The mice received 0.5-ml i.p. injections of phosphate-buffered saline (PBS; control) or dosages of ENU (Pflatz and Bauer, Stanford, CT) ranging from 5 to 75 mg/kg body weight in PBS each day for 5 consecutive days. Repeat and additional experiments at South Dakota State University utilized a different shipment of ENU received 6–8 months prior to use; this older stock of ENU apparently did not have the same activity as the stock used at Sloan-Kettering Research Institute, since an approximately 50% higher dose was needed to produce the same biological effects. Injections were made within 1 h after preparation of the ENU solutions.

### Sample Preparation

Twenty-eight days following the last chemical exposure, the mice were killed by cervical dislocation and weighed. The testes were surgically removed, weighed, and placed into Hanks Balanced Salt Solution (HBSS) at 4°C. At least one testis from each animal was minced with scissors to form a cellular suspension that was passed through 53-μm nylon mesh (Tetko, Inc., New York, NY) wedged between the end of a tuberculin syringe and the plastic protective cap (tip removed with wire cutter). The caudal epididymides were also removed, placed into TNE (0.01 M TRIS, 0.15 M NaCl, and 1 mM EDTA, pH 7.4), minced with scissors, and the suspension was pipetted in and out of a Pasteur pipette several times prior to filtering through 153-μm nylon mesh, as above.

After aliquots of epididymal sperm were removed for AO staining and morphology assays, the remainder of each dosage group was pooled and prepared for thermal denaturation of sperm nuclei by the following steps, all done at 0–4°C. Sperm were suspended in a total volume of about 12 ml TNE and pelleted at 12,500 × g for 10 min. The process was repeated and the resulting pellet resuspended in 3.6 ml of TNE buffer and transferred to a Falcon plastic test tube (No. 3033) which was immersed in an ice water slurry.

The sample was then sonicated with a Bronwill Biosonik IV Sonicator (VWR Scientific Inc., Minneapolis, MN) equipped with a 3/8-in diameter probe and operating at a power setting of 50 on the low-range power; alternatively, a model 185 Bronson Sonifier was used at a power scale of 3.5 with the same results. This sonication step raises the temperature of the sonicate from 4° to 12°C. After 30 sec of cooling in the same ice bath, the cells were sonicated at the same power range for an additional 30 sec. The sonication procedure disrupts somatic cells and separates sperm heads from tails; electron micrographs of these sperm nuclei show they were intact with partially disrupted nuclear membranes (data not shown). The sonicate was admixed with 1.2 ml of 60% sucrose (w/w) in 0.01 M TRIS-HCl (pH 7.4) and 2 mM EDTA, layered over 9 ml of the same sucrose solution in 16-ml Sepcor polycarbonate tubes with caps (Separation Science Corp., Stratford, CT), and centrifuged at 27,500 × g in a Sorvall HB4 rotor for 1 h. After the supernatant was removed by vacuum aspiration, the pellet was resuspended in 1.0 ml of 0.15 M NaCl, 5 mM $MgCl_2$, and 0.02 M TRIS-HCl (pH 7.4), forcefully expelled from a Pasteur pipette into a glass test tube containing 9.0 ml of an ice cold 1:1 mixture of 70% ethanol and acetone, and stored at −20°C (8).

### Cell Staining

#### Acridine orange (AO) staining of fresh cells

**Two-step AO staining.** Within an hour after sample preparation, testicular cells and epididymal sperm were stained by the two-step AO technique (5) and measured by flow cytometry; briefly, about 2–4 × $10^5$ cells in 0.20-ml buffer were admixed with 0.40 ml of 0.1% (v/v) Triton X-100, 0.08 N HCl, and 0.15 M NaCl for 30 sec, followed by the addition of 1.2 ml AO staining solution [0.20 M $Na_2HPO_4$, 0.1 M citric acid buffer (pH 6.0), 1 mM EDTA, 0.15 M NaCl, and 6.0 μg/ml chromatographically purified AO (Polysciences, Inc., Warrington, PA)].

The differential staining of double-stranded DNA versus single-stranded nucleic acids (DNA or RNA) is due to the metachromatic properties of AO: the dye fluoresces green ($F_{530}$) when intercalated into double-stranded nucleic acids (31) and exhibits red ($F_{600}$) fluorescence when bound to single-stranded polymers (3,25,26). AO stained normal, mature sperm fluoresce primarily green but at about one-tenth the level of so-

matic cells due to their haploid DNA content and a high level of chromatin condensation that restricts the dye binding to DNA (9,17). Because mature sperm do not contain any significant amounts of RNA, the differential staining of sperm reflects predominantly a ratio of double- to single-stranded DNA.

For FCM measurements of testicular samples, red and green photomultiplier tube (PMT) gains were initially set to include all cell types ranging from tetraploids to elongated spermatids. The sample was then remeasured at higher PMT gains to include only round, elongating, and elongated spermatids. Samples were measured from at least three randomly chosen mice in each group. Epididymal sperm were also stained in exactly the same way and measured by flow cytometry, recording on list mode red and green fluorescence or by use of a computer program converting the fluorescence values to total fluorescence and $\alpha_t$ $\{\alpha_t$ = red/(red + green)$\}$.

**One-step AO staining.** Isolated nuclei were stained directly with the AO staining solution described below for thermal denaturation. For staining whole sperm, 0.1% Triton X-100 was added to the staining solution to permealize the cell membranes (5).

### Thermal Denaturation of Fixed Nuclei

After storage at −20°C for time periods of overnight to several months, the fixed nuclei from each dosage group were pelleted at 4800 × g for 10 min. Following careful aspiration of the supernatant, nuclei were resuspended in 12 ml of "heating buffer" consisting of $2 \times 10^{-3}$ M sodium cacodylate, $10^{-4}$ M EDTA and 40% ethanol (pH 6.0). After 30 min to allow for equilibration, each nuclear suspension was transferred to a Sorvall glass test tube and centrifuged for 10 min at 16,000 × g in a Sorvall HB4 rotor; the pellets were again resuspended in 1 ml of heating buffer. For the unheated sample, a 0.20-ml aliquot was admixed with 2.0 ml of staining buffer consisting of 0.15 M NaCl, 5 mM $MgCl_2$, 0.02 M TRIS-HCl (pH 7.4), and 8.0 μg/ml AO (8), and measured after 3 min by FCM. For the heated sample, an aliquot with increased volume (0.40 ml to compensate for loss of volume and nuclei sticking to the test tube during the heating process) of suspended nuclei was transferred to a Falcon plastic test tube (No. 3033). This tube was placed into a boiling water bath for 5.0 min, then cooled in an ice water slurry for 15 sec prior to the addition of 2.0 ml of the above AO staining solution. Samples were measured 3 min later by FCM.

### Flow Cytometry

Samples were measured either in an Ortho FC200 Cytofluorograf (Ortho Diagnostics, Inc., Westwood, MA) interfaced to a Nova 1220 minicomputer (located in the Department of Investigative Cytology, Sloan-Kettering Research Institute) or in a Cytofluorograf II interfaced to an Ortho Diagnostics 2150 data handling system (located in the Department of Chemistry, South Dakota State University). Both flow cytometers were equipped with a Lexel 100 mW argon ion laser. Some experiments were done once at SKI and repeated at least once, in addition to new experiments, at SDSU. Data shown in Figures 1–8 and 10–14 were derived at SKI; data shown in Figures 9, 15, 16 and Tables 1 and 2 were derived at SDSU.

Green and red fluorescence values were measured for each cell and the ratio of red/(red + green) fluorescence was determined by software protocols written for that purpose. The data were based on 5,000 to 10,000 cells per sample.

### Enzyme Digestions

Sperm nuclei were isolated and purified through a sucrose gradient as described above, resuspended in 0.15 M NaCl, 5 mM $MgCl_2$, and 0.02 M TRIS-HCl (pH 7.4), then split into aliquots that were either: 1) fixed in 70% ethanol:acetone (1:1), 2) stained with AO by the one- or two-step method, or 3) pelleted again and resuspended in an appropriate buffer for enzymatic digestion. The following solutions were used for enzymatic digestion: 1) pancreatic ribonuclease A (Cooper Biomedical, Inc., Malvern, PA), $1.5 \times 10^3$ units per ml in HBSS; alternatively, $1.5 \times 10^3$ RNAse units/ml were added to a suspension of whole cells after staining by the two-step AO procedures; 2) bovine pancreatic DNAse I, chromatographically purified (Sigma Chemical Co., St. Louis, MO), 200 Kunitz units per ml in HBSS; 3) nuclease $S_1$ (Cooper Biomedical, Inc.), $1.5–2.0 \times 10^3$ units per milliliter in 0.06 M sodium acetate (pH 4.6), 0.10 M NaCl and 2 mM $ZnCl_2$; and 4) combination of DNAse I and RNAse at concentrations listed above in HBSS. Enzymatic digestion of nuclei ($1–2 \times 10^6$/ml) was done at 37°C for 1–3 h as detailed below.

### Electron Microscopy

Small testicular biopsies excised with a razor blade, and pelleted epididymal sperm samples were fixed with 2.5% glutaraldehyde in PIPES (Polysciences, Inc., Warrington, PA) buffer (4°C) for 1.5 h, rinsed briefly with buffer, and then post-fixed with 2% osmium tetroxide for 1 h. Following a water rinse, the samples were dehydrated with a graded series of ethanol, followed by propylene oxide and embedding in Epon 812 by routine procedures. After polymerization of the Epon at 37°C overnight, 60°C for 1 day and 90°C for an additional day, thin sections were cut with a Porter-Blum MT2 Sorvall ultramicrotome equipped with a diamond knife. These sections were stained with 0.5% uranyl acetate in absolute methanol followed by lead citrate and then examined in a JOEL 100B electron microscope operating at 80kV.

### Sperm Head Morphology

An aliquot of each epididymal sperm suspension was admixed (10:1) with freshly filtered 1% Eosin Y ($H_2O$). After 30 min, two smears were made for at least three samples per group. After air drying, slides were briefly rinsed in methanol to remove excess stain, air dried again, and mounted in Permount mounting medium. For each suspension, a minimum of 1,000 sperm heads were scored by the morphology criteria of Wyrobek and Bruce (42) using a light microscope under a 100 × oil objective lens (total 1,000 ×) and a blue-green filter.

## RESULTS

### Body and Testicular Weights

Figure 1 shows that exposure to cumulative dosages of ENU ranging from 0 to 250 mg/kg body weight did not have a significant effect on total body weight 28 days after the last exposure. In contrast, the chemical exposure induced an approximate 10% decrease of testicular weight at the lower cumulative dosages (25 and 50 mg/kg) and a greater than 50% decrease at the highest concentration (250 mg/kg).

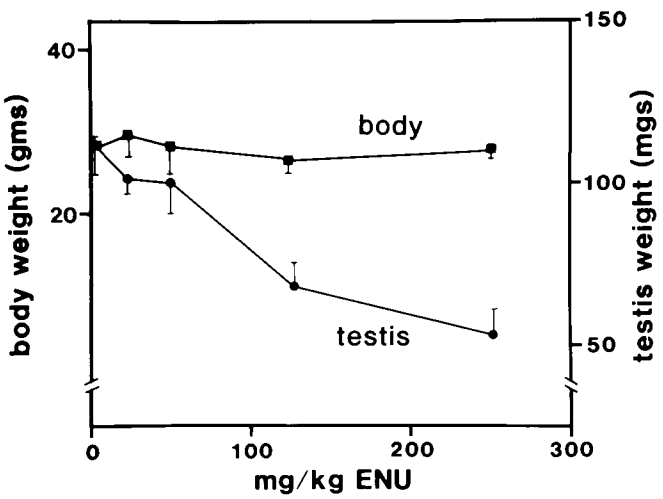


FIG. 1. Effects of ENU on mouse body and testicular weights. Each point is the mean weight (± SD) from seven individual animals 28 days after last exposure. For the points at 0 dosage, the shorter SD bar corresponds to body weight.

### Testicular Fine Structure

The destructive action of ENU on testicular structure can be seen in Figure 2B and compared to testicular structure of a control mouse in Figure 2A. The seminiferous tubules of ENU treated mice demonstrated a dramatic decrease of spermatids and maturing sperm. For the cell types remaining however, this ultrastructural analysis did not reveal any specific cytological damage at 28 days post-treatment.

### FCM Analysis of Testicular Samples

Testicular cell suspensions from at least three randomly chosen mice per group were stained by the two-step AO method and measured by flow cytometry to determine the correlated red and green fluorescence levels as shown in Figure 3. Incubation of fresh cellular suspensions with Type VII collagenase, Type XI protease and/or DNAse I (all enzymes from Sigma Chemical Co., St. Louis, MO) did not significantly change the cellular staining distributions (data not shown). Note in both the scattergrams and frequency histograms the significant shift in the ratio of cell types as a consequence of chemical exposure. Figure 4 is a plot of computer derived values showing a significant relative decrease in 1N cells and a concomitant relative increase in the ratio of 2N and 4N cells.

Four types of 1N cells can be discerned by the two-step AO technique in contrast to only three seen by DNA specific stains (33). In this experiment, the small percentage of mature testicular sperm were excluded and only round, elongating and elongated spermatids were evaluated. In order to more accurately determine the relative percentage of 1N cell types, the red and green PMT gains were increased after each measurement represented in Figure 3. Figure 5 shows the scattergrams and frequency histograms for these measurements. The control sample (0 mg/kg) demonstrates the predominant round spermatid population and a minor population with similar green but reduced red fluorescence, shown previously (14) to represent DNA and RNA, respectively. Note the dramatic loss of elongated spermatids in response to ENU exposure (Fig. 5,6).

### Effect of ENU on Caudal Epididymal Sperm

**Sperm head morphology.** Using the technique of Wyrobek and Bruce (42), sperm nuclei (including those heads broken free from tails) were classified as having either normal or abnormal morphology. The mean values of measurements from three or more mice per group show a near linear response to dosage (Fig. 7) with an increase from a 5% background to 6% at the lowest dosage and 21% at the highest dosage. In this experiment, a great amount of variation existed between animals at the highest concentration. A repeat experiment (data not shown but represented in Figs. 15 and 16 and Tables 1 and 2) showed a much lower standard deviation of the percentage of abnormal sperm: a) control, 2.5 ± 0.5; b) 250 mg/kg, 10.5 ± 2.9; c) 375 mg/kg, 20.8 ± 1.5.

### Electron Microscopy of Epididymal Sperm

Epididymal sperm were examined by transmission electron microscopy to determine whether ENU induced alterations of chromatin structure could be visualized. Observation at magnifications up to 100,000 × of at least 50 sperm isolated from mice treated with 125 and 250 mg/kg ENU showed no visible alterations of nuclear chromatin structure relative to control, untreated mice. Figures 8A and B are electron micrographs of sperm from treated and untreated animals, respectively. In both cases, the nuclear chromatin structure appears similar, i.e., is amorphous in character due to the highly condensed nature of sperm chromatin, upon which ENU exposure had no visible morphological effect.

### FCM Analysis of Caudal Epididymal Sperm

**Differential AO stainability of fresh sperm, fresh and fixed nuclei.** Figure 9 shows the differential stainability of whole fresh epididymal sperm, fresh and fixed isolated nuclei stained by the one- or two-step AO staining procedure. Note that fresh isolated sperm nuclei have slightly higher green, red, total fluorescence and $\alpha_t$ values than do whole sperm. Fluorescence measurement of a sperm cell is highly sensitive to the orientation of the head, due to the high refractive index and flat shape of the nucleus. When analyzed in a flow cytometer with

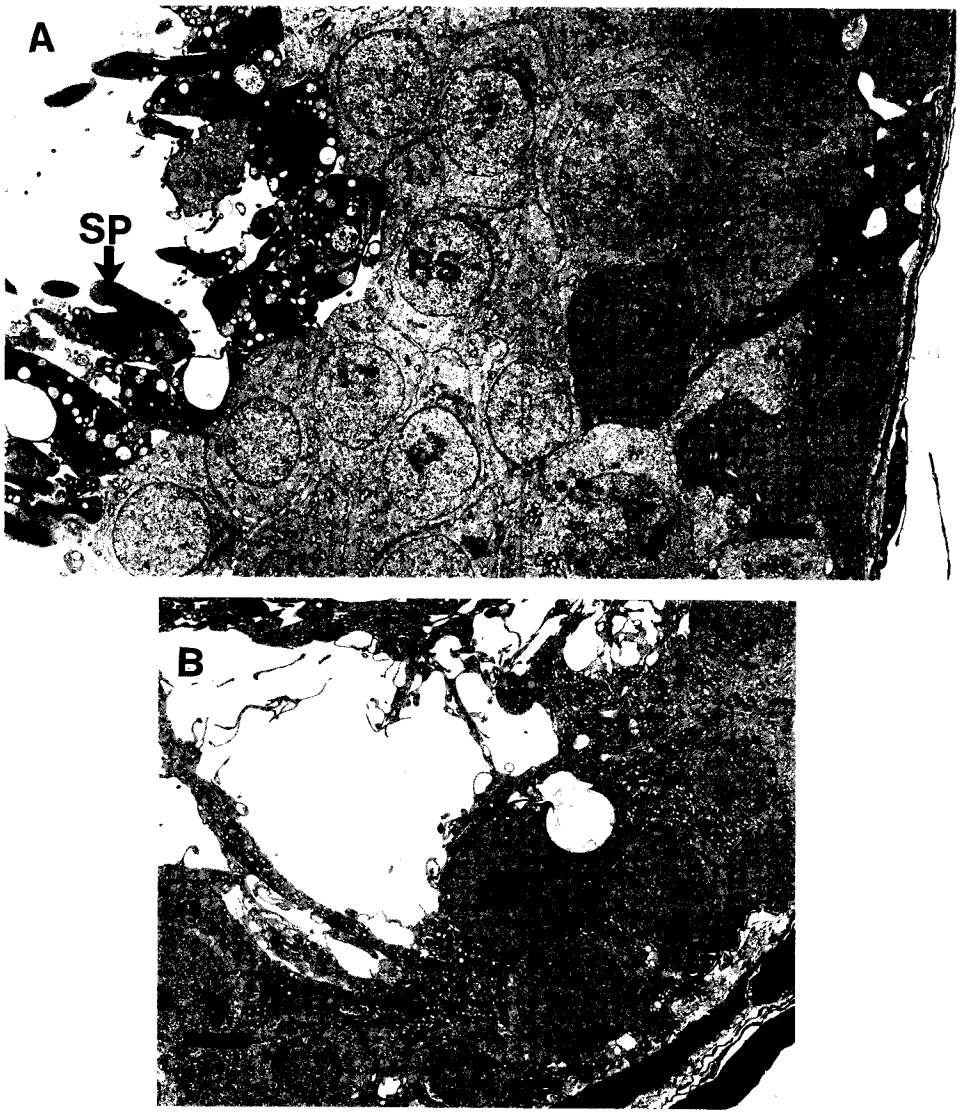


FIG. 2. Effects of ENU on testicular fine structure. A) control; B) exposed to 250 mg/kg ENU. (S) spermatogonium, (PS) primary spermatocyte, (RS) round spermatid, (SP) sperm. Bars equal 5 $\mu$m.

orthogonal geometry, varying orientations among cells result in an elongated scattergram signal, as described by Gledhill et al. (19) and noted in Figure 12. Our comparisons of green fluorescence frequency histograms for whole sperm and isolated nuclei indicate that alterations in the orientation of nuclei versus intact cells at the time of measurement likely cause the increase in fluorescence values. It is also possible that there is slightly greater accessibility of AO to the DNA in isolated nuclei than in whole sperm, which would contribute to higher fluorescence values.

The two-step AO procedure, which includes exposure to 0.08 N HCl treatment for 30 sec, increases green, red, and total fluorescence by a factor of about 1.3 relative to the one-step. The increase of green and red fluorescence is apparently due to acid displacement of proteins and moderate DNA denaturation.

Fixation of nuclei in 70% ethanol:acetone (1:1) followed by rehydration (as described in Materials and Methods) reduces green, red, and total fluorescence of two-step AO stained samples by 36, 66, and 41% respectively, relative to unfixed nuclei.

The $\alpha_t$ values of whole sperm and isolated nuclei are similar, whereas for fixed nuclei they are somewhat reduced due to a greater percentage drop in red than green fluorescence.

## Effect of ENU on AO Stainability of Fresh Epididymal Sperm

Epididymal sperm were stained by the two-step AO technique and measured by FCM. For convenience of

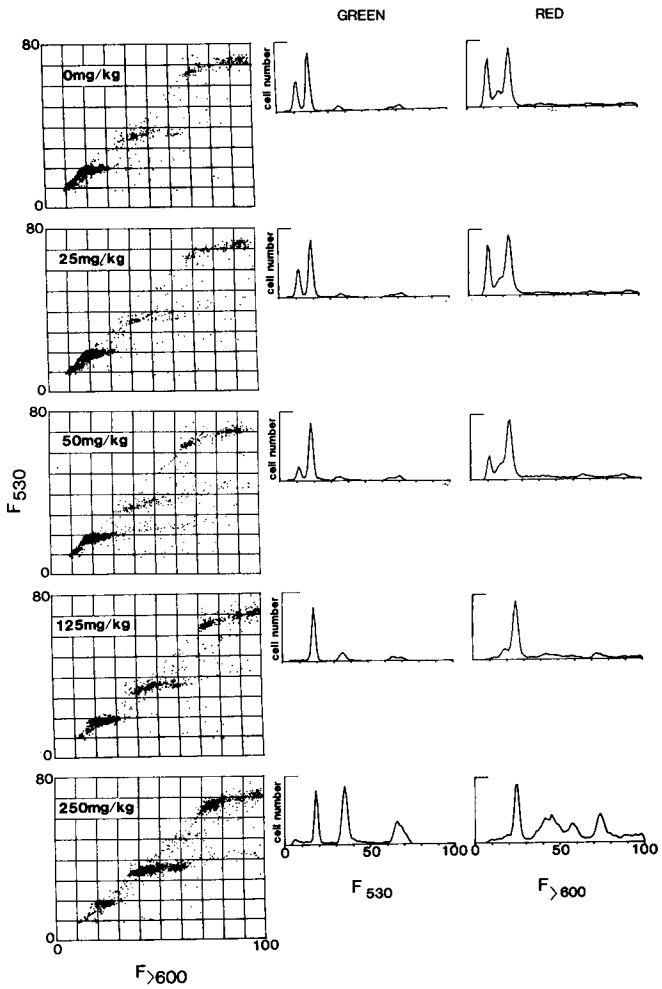


FIG. 3. Computer-drawn two-parameter ($F_{530}$ versus $F_{>600}$) scattergrams of the distribution of individual AO-stained testicular cells from control and ENU-treated mice. To the right of each scattergram are the green and red fluorescence frequency distribution histograms. Green fluorescence channels correspond to the tetraploid (62–75); diploid (32–40); round and elongating spermatids (15–22); elongated spermatids (9–15). Epididymal sperm would be represented at about channel 5.

analysis, the measurements were displayed as total fluorescence versus $\alpha_t$ which avoids the vertical distribution being tilted to the right as seen when green versus red fluorescence is displayed. Thus, this distribution permits a definition of vertical and horizontal limits for normality and abnormality of staining.

Two shifts in the sperm population are evident from the scattergrams shown in Figure 10. First, in a dose-dependent fashion, the populations shifted to higher $\alpha_t$ values indicative of a higher ratio of single-stranded DNA (8,25). Addition of 1,000 units/ml of RNAse to these detergent AO treated samples did not significantly change the staining pattern after 20 min incubation (data not shown). Also, incubation of ethanol-fixed, rehydrated samples with RNAse for 20 min did not significantly change the staining profile, suggesting that these altered patterns are not due to residual RNA in the cell. Light microscopy did not reveal an increased presence of cytoplasmic droplets. (See below for additional enzymatic digestion experiments.)

The second apparent shift was the appearance of a population with a lower total fluorescence, ranging between channels 15 and 25 on the ordinate. A small percentage of this cell type is seen in the control sample and an increasing percentage with higher ENU exposure.

Figure 11 is a plot of the computer-derived coefficient of variation (CV) of the $\alpha_t$ values from the experiment in Figure 10. Note the significant increase in the CV of $\alpha_t$ in a dose-response manner.

**Effect of ENU on resistance of sperm chromatin to thermal stress.** The effect of ENU on sperm chromatin structure was also evaluated by subjecting isolated nuclei to thermal stress and measuring red and green fluorescence in AO stained nuclei. Figure 12 displays a series of scattergrams showing two independent measurements of unheated and heated nuclei stained with AO and measured by FCM. Note the high degree of repeatability between the two sets of measurements. At the higher concentrations of ENU, it is obvious that there is a wider distribution in the AO staining patterns in the heat-treated samples. This change, expressed as frequency histograms of $\alpha_t$, can be seen in Figure 13. Figure 14 expresses the changes in the coefficient of variation of $\alpha_t$. In this experiment, the mean $\alpha_t$ did not significantly vary; however, the CV significantly increased as dose increased. Note the measurable increase of the CV of $\alpha_t$ at the lowest dosage of ENU.

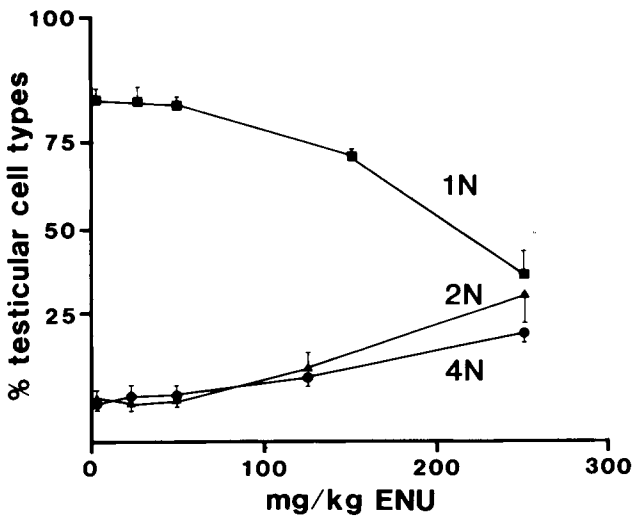


FIG. 4. Effect of ENU on the relative proportion of 1N–4N cell types present in testicular cell suspensions. The means and standard deviations were derived from measurements (experiment in Fig. 3) on cells from one testis obtained from each of three randomly chosen individual animals per group.

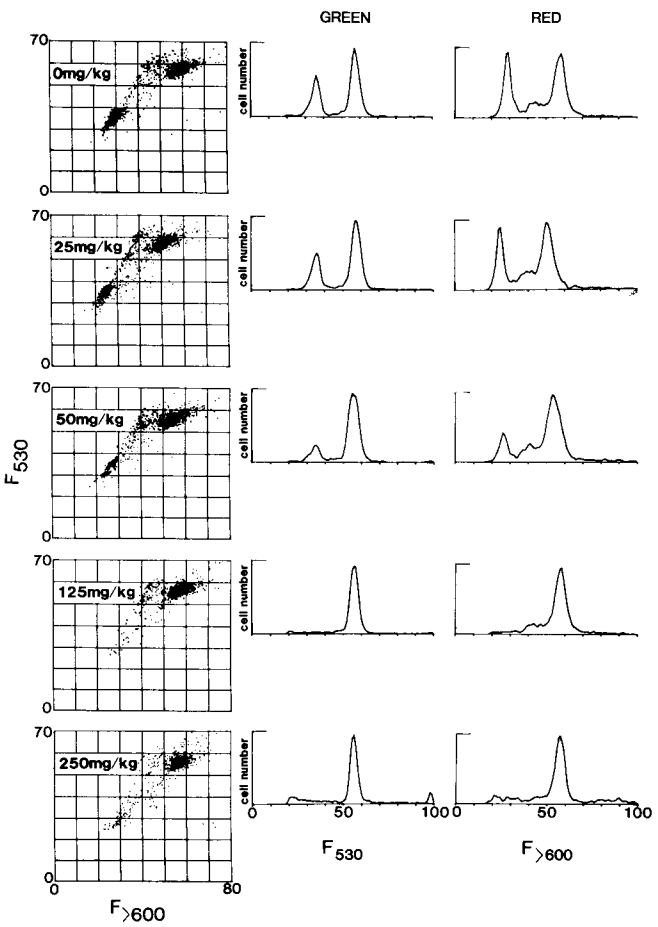


FIG. 5. Computer-drawn scattergrams of the distribution of individual 1N testicular cells from control and ENU treated mice according to their red and green fluorescence intensities after staining with AO; to the right of each scattergram are the green and red fluorescence frequency distribution histograms.

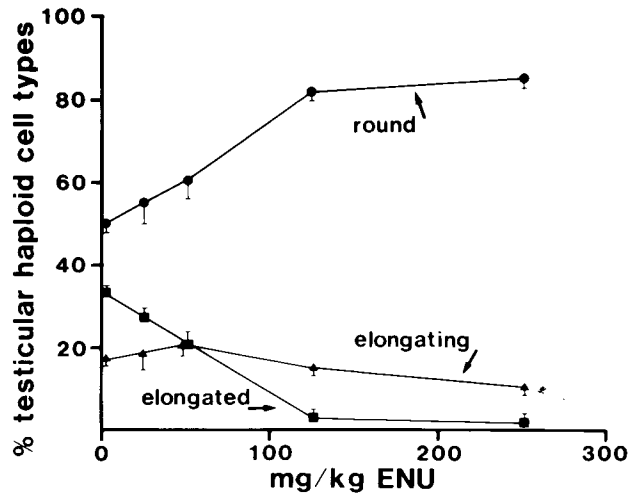


FIG. 6. Effect of ENU on the percent of haploid cell types present in testicular cell suspensions. The percentages were derived by computer analysis of the data in Figure 5. Each point represents the mean of measurements on cells from one testis obtained from each of three randomly chosen individual animals per group. The vertical lines show the standard deviations.

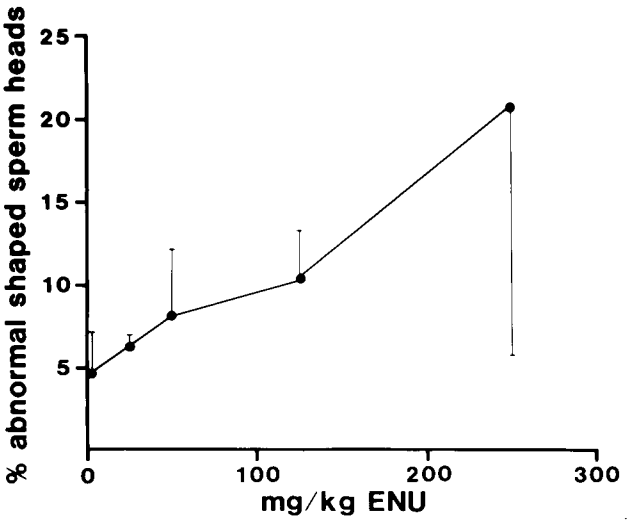


FIG. 7. Effects of ENU on caudal epididymal sperm head morphology. A minimum of 350 sperm heads from each of three slides representing three mice were scored for normal/abnormal morphology. Each point represents the mean of the three slides; the vertical lines show the standard deviations.

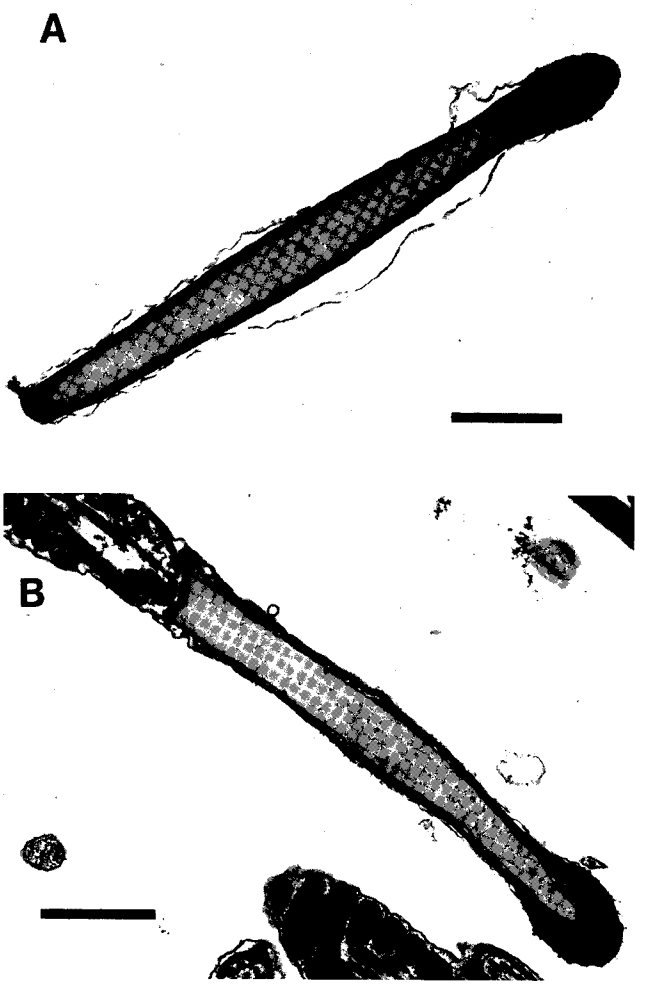


FIG. 8. Electron micrographs of thin sections of caudal epididymal sperm isolated from: (A) control mouse, or (B) a mouse exposed to 250 mg/kg ENU. Bars equal 1 $\mu$m.

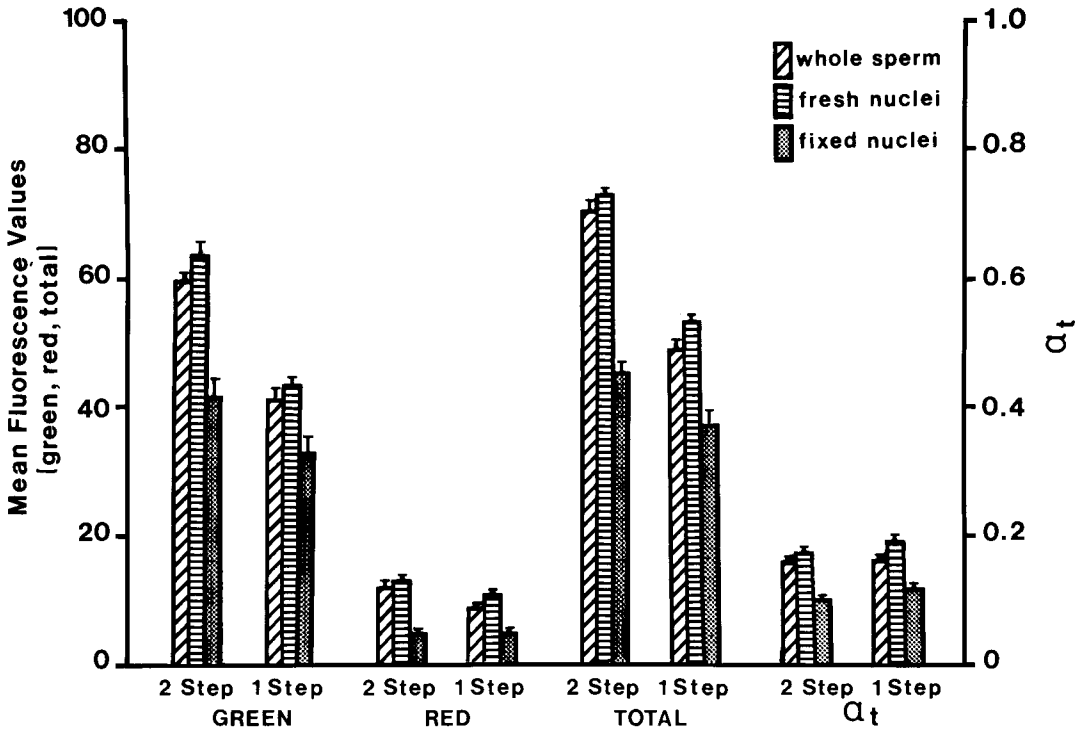


FIG. 9. Red and green fluorescence mean values of whole sperm, fresh and fixed nuclei after staining by the one- or two-step AO method. The line above each bar indicates the standard deviation. For whole sperm n = 4 (2 measurements on each of 2 samples); for isolated nuclei n = 2 (2 measurements on one sample).

Table 1
*Mean Fluorescence Values of Purified Unfixed Mouse Caudal Epididymal Sperm Nuclei Following Incubation With or Without RNAse and DNAse I*

| ENU dosage[a] | Enzyme treatment | Green ($F_{530}$) | Red ($F_{>600}$) | Total ($F_{530} + F_{>600}$) | $\alpha_t$ ($F_{>600}/F_{530} + F_{>600}$) | |
|---|---|---|---|---|---|---|
| 0 | No enzyme | 56.8[b] | 18.5[b] | 75.3[b] | 0.25[c] | 5.5[d] |
| | RNAse | 56.7 | 17.7 | 74.4 | 0.24 | 6.6 |
| | | (− 0.2)[e] | (− 4.3) | (− 1.2) | (− 4.0) | |
| | DNAse I | 49.3 | 28.3 | 77.6 | 0.36 | |
| | | (− 13.2) | (+ 53.0) | (+ 3.1) | (+ 44.0) | |
| | DNAse I + RNAse | 46.5 | 35.6 | 82.1 | 0.43 | |
| | | (− 18.1) | (+ 92.4) | (+ 9.0) | (+ 72.0) | |
| 250 | No enzyme | 54.0 | 16.6 | 70.6 | 0.23 | 10.3 |
| | RNAse | 56.3 | 17.6 | 73.9 | 0.24 | 10.7 |
| | | (+ 4.3) | (+ 6.0) | (+ 4.7) | (+ 4.4) | |
| | DNAse I | 48.2 | 33.0 | 81.2 | 0.40 | |
| | | (− 10.7) | (+ 98.8) | (+ 15.0) | (+ 73.9) | |
| | DNAse I + RNAse | 48.5 | 31.7 | 80.2 | 0.39 | |
| | | (− 10.2) | (+ 91.0) | (+ 13.6) | (+ 69.6) | |
| 375 | No enzyme | 54.2 | 18.2 | 72.4 | 0.25 | 12.2 |
| | RNAse | 55.6 | 20.2 | 75.8 | 0.26 | 13.3 |
| | | (+ 2.6) | (+ 11.0) | (+ 4.7) | (+ 4.0) | |
| | DNAse I | 48.5 | 29.6 | 78.1 | 0.38 | |
| | | (− 10.5) | (+ 62.6) | (+ 7.9) | (+ 52.0) | |
| | DNAse I + RNAse | 46.9 | 33.9 | 80.8 | 0.42 | |
| | | (− 13.5) | (+ 86.3) | (+ 11.6) | (+ 68.0) | |

[a]mgENU/kg of body weight.
[b]Mean channel of frequency histogram; range: 0–100.
[c]Range: 0–1.0.
[d]CV of $\alpha_t$.
[e]Values in parentheses are percentage change from "no enzyme" treatment of same ENU dosage.

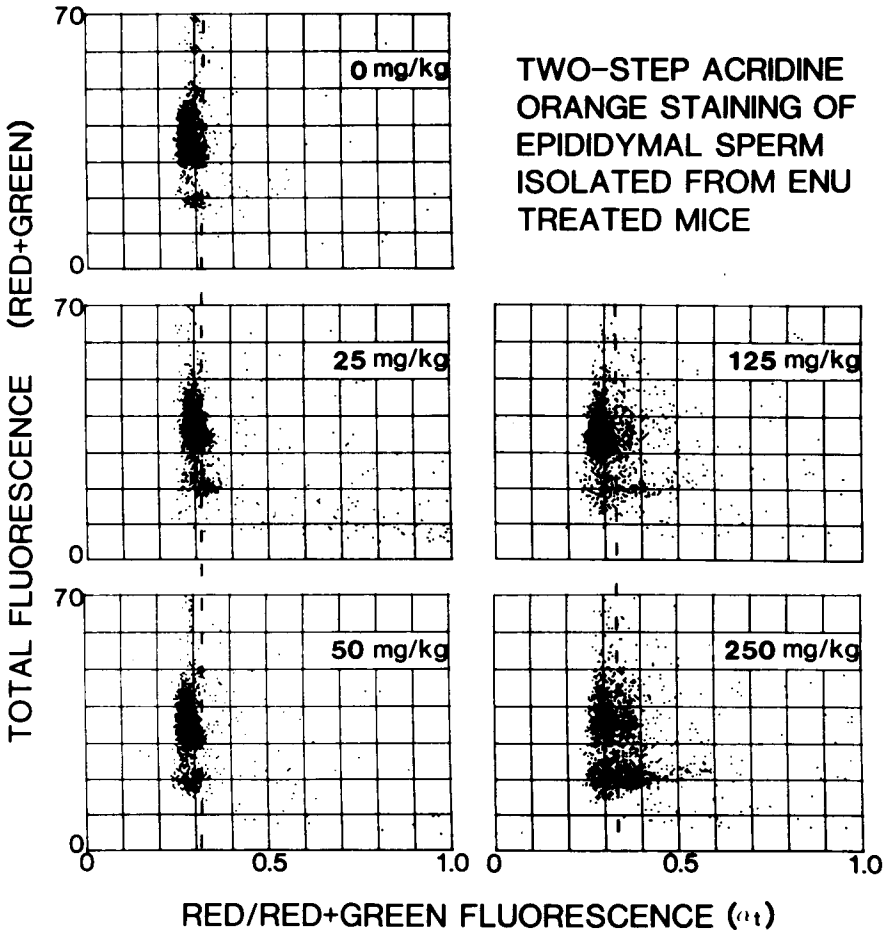


FIG. 10. Relationship between red and green fluorescence emission of epididymal sperm stained by the two-step AO procedure and the exposure level of ENU.

**Effects of RNAse and DNAse I digestion on AO stainability of fresh epididymal sperm nuclei from mice exposed to ENU.** Figure 15 and Table 1 show the effects of various nuclease incubations on the fluorescence of freshly isolated sperm nuclei stained by the two-step AO method. In agreement with the data in Figure 12, the mean $\alpha_t$ of isolated nuclei did not change significantly in response to ENU; the CV of $\alpha_t$, however, increased in a dose-response relationship. RNAse incubation alone did not significantly change green, red, or total fluorescence values nor $\alpha_t$ mean or CV values. Thus, the increase of CV of $\alpha_t$ in response to ENU was not significantly influenced by RNAse incubation; this agrees with the lack of effect on red fluorescence of RNAse treatment of whole sperm stained by the two-step AO procedure (as noted for experiment in Fig. 10).

As seen in Figure 15 and Table 1, and as consistently observed in other unpublished data, DNAse I pretreatment of isolated nuclei or permeablized cells reduced green fluorescence and increased red fluorescence. For dosage groups of 0, 250, and 375 mg/kg the mean green fluorescence decreased by 3–15% and the mean $\alpha_t$ increased by 44–74%. Thus, the major change after DNAse I treatment was an increase of red fluorescence. To investigate whether this increase might be due to DNAse digestion making the dye more accessible to hypothetical intranuclear RNA, RNAse was added to the DNAse I incubation mixture and incubation was continued for another hour, after which time samples were measured by two-step AO staining. For all three dosage groups, no decrease of red fluorescence or $\alpha_t$ was observed below that of the DNAse I incubation sample alone; in the 0 and 375 mg/kg dosages, these values actually increased, most likely due to continued DNAse I digestion.

To further investigate the nature of red fluorescence after thermal stress, fixed nuclei were heated at 100°C for 5 min by our routine procedure and then pelleted and resuspended in nuclease $S_1$ buffer with or without nuclease $S_1$. After incubation for 2 h at 37°C, aliquots were removed and stained with the AO staining mixture routinely used for heated nuclei. Note in both Figure 16 and Table 2 that nuclease $S_1$ digestion under these conditions did not reduce red fluorescence; in fact, all measurements showed an increase of green and red fluorescence mean values. The nuclease $S_1$ preparation was not guaranteed to be free of protease activity, and other studies have shown $S_1$ preparations to have protease activity (23). Protease digestion occurring during $S_1$ incubation would be expected to contribute to increased green and red fluorescence (9).

Table 2
*Mean Fluorescence Values of Purified Fixed Mouse Caudal Epididymal Sperm Nuclei After Thermal Denaturation and Subsequent Incubation With or Without $S_1$ Nuclease*

| ENU Dosage [a] | Enzyme treatment | Green ($F_{530}$) | Red ($F_{>600}$) | Total ($F_{530} + F_{>600}$) | $\alpha_t$ ($F_{>600}/F_{530} + F_{>600}$) |
|---|---|---|---|---|---|
| 0 | No enzyme | 40.5[b] | 11.0[b] | 51.5[b] | 0.21[c] |
| | $S_1$ Nuclease | 51.2 | 13.8 | 65.0 | 0.21 |
| | | (+ 26.4)[d] | (+ 25.5) | (+ 26.2) | (0) |
| 250 | No enzyme | 44.3 | 13.5 | 57.8 | 0.23 |
| | $S_1$ Nuclease | 50.4 | 17.2 | 67.6 | 0.25 |
| | | (+ 13.8) | (+ 27.4) | (+ 17.0) | (+ 8.7) |

[a]mgENU/kg of body weight.
[b]Mean channel of frequency histogram; range: 0–100.
[c]Range: 0–1.0.
[d]Values in parentheses are percentage change from "no enzyme" treatment of same ENU dosage.

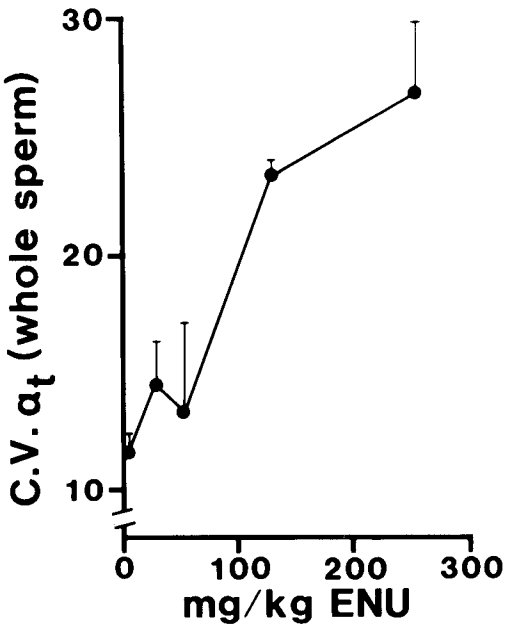


FIG. 11. Relationship between the computer derived coefficient of variation (CV) of $\alpha_t$ of two-step AO stained whole epididymal sperm and dosage of ENU exposure (from experiment in Fig. 10). Each point represents the mean of measurements on sperm isolated from three randomly chosen individual mice per group. The vertical lines show the standard deviations.

## DISCUSSION

The effects of ENU, a powerful carcinogen and mutagen (24,36), on mouse testicular function have been measured by classical criteria using light and electron microscopy and compared with flow cytometric evaluation of the same samples. ENU had no significant effect on body weights of the mice, whereas it caused up to a 50% loss of testicular weights, indicating the sensitivity of the testis to the action of this chemical.

Loss of testicular weight is reflected in the specific loss of haploid cells as determined by morphological and FCM measurements. These FCM measurements require only several minutes per fresh testicular sample; thus, an analysis of chemically induced alterations of testicular cell type ratios can be rapidly obtained. In contrast to single parameter FCM measurements of DNA stained testicular cells that identify only three to four cell types, the two-step AO technique identifies five or more populations in a testicular cell preparation (14). Elongated, elongating, and round spermatids, as well as mature sperm, can easily be distinguished due to differences in RNA content and DNA stainability. The diploid population is considered here as only one of the five poulations, but it contains both germ and somatic cells. It is apparent from the F > 600 (RNA) frequency histogram in Figure 3 that the diploid population (channels 32–60; 250 mg/kg) consists of two major populations that could be sorted for further analysis.

Examination of the data shown in Figures 5 and 6 revealed a dramatic loss of haploid germ cells from the testes of ENU treated mice. Rodriguez et al. (34) have concluded that ENU damages spermatogonia but not spermatocytes, spermatids, or spermatozoa and that the loss of cells with time is only a result of damage to spermatogonia. If so, then the damage apparently includes the mechanisms involved in differentiation from a round spermatid to an elongated spermatid. Alternatively, ENU may also damage differentiating spermatogonia and spermatids, as evidenced by mutations recovered among the progeny of males exposed to ENU, at which time the fertilizing sperm would have been differentiating spermatogonia or early spermatocytes (35) or spermatids (32).

ENU caused a significant increase in caudal epididymal sperm head morphology abnormalities similar to levels induced by other strong mutagens (44). The mechanisms responsible for these changes are not understood, nor are the relationships between genetic controls of sperm shaping in nontreated animals and abnormalities induced by chemical treatment. Furthermore, the effect of altered head shapes on fertility is unclear, since not only do certain inbred strains of mice have different and specific head shapes (2), but lines vary widely in frequency of abnormal sperm head shapes, ranging from 3 to 65% in one survey of inbred strains and $F_1$ hybrids (41). Hybrids generally have lower levels of abnormalities than either parental line. Also, sperm head shape is not a direct reflection of the integrity of the chromosome

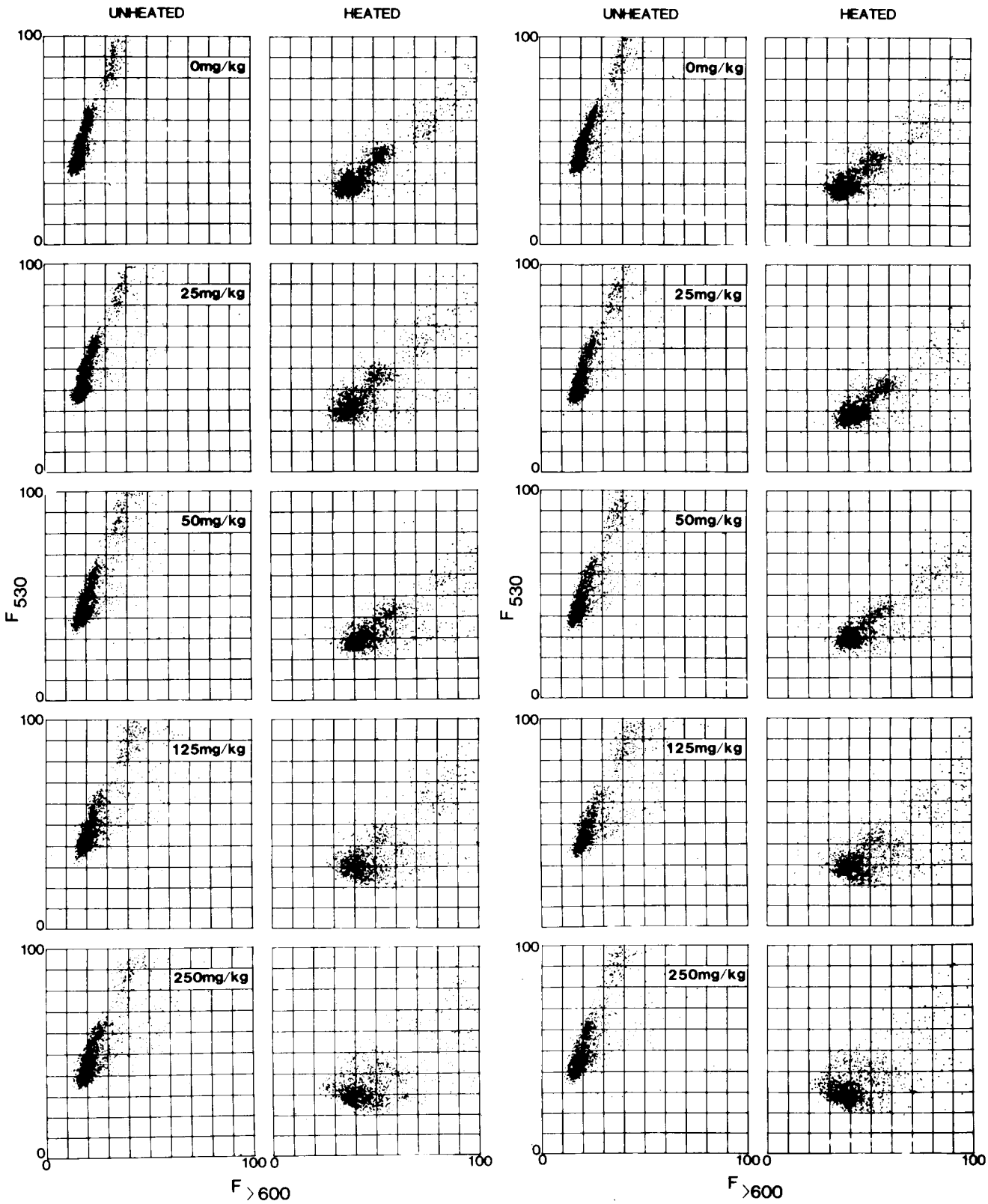


FIG. 12. Effect of thermal denaturation on mouse sperm nuclear DNA in situ following exposure to ENU. The five samples (pool of sperm nuclei from 4 mice/group) were rehydrated and then randomly selected to measure the AO-stained unheated sample followed by measuring an aliquot of the same sample after heating. After the five samples were measured, they were again randomly selected to be measured before heating and after heating. The total elapsed time after rehydration and the last measurement was about 4 h, showing the stability of the nuclei in buffer. Note the reproducibility of the staining patterns.

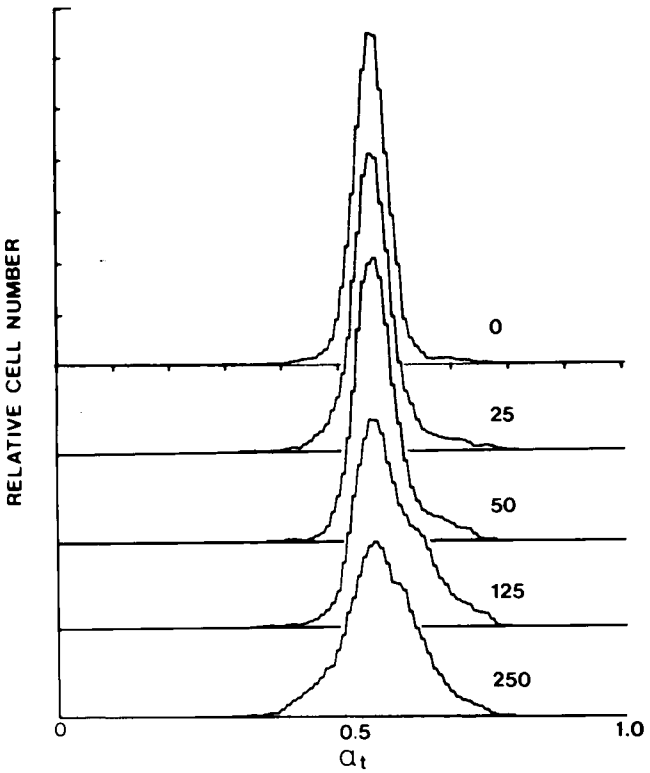


FIG. 13. Effect of ENU on mouse sperm $\alpha_t$ distributions; $\alpha_t$ frequency histograms were computer generated from the data represented in Fig. 12 (measurement No. 1, heated samples).

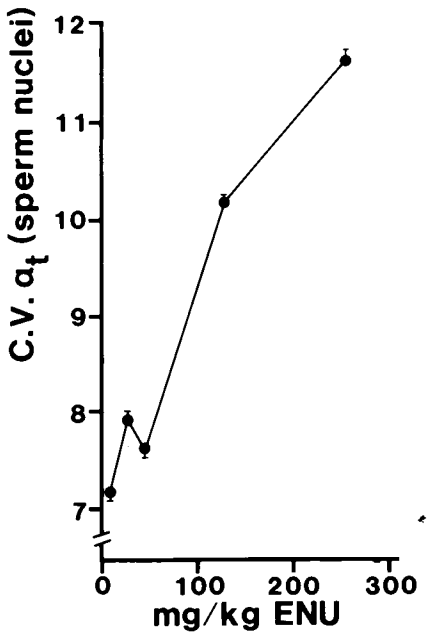


FIG. 14. Relationship between the computer derived coefficient of variation of $\alpha_t$ of heated and AO stained epididymal sperm nuclei and exposure level to ENU (from experiment in Fig. 12). Each point represents the mean of three separate measurements of the pooled sperm nuclei. The vertical lines show the standard deviations.

complement, since the frequency of abnormal sperm head morphology has been shown not to be proportional to the frequency of sperm known to contain translocated chromosomes and partial or total chromosomal duplications and deficiencies (41). Perhaps related to these observations, previous studies on the effects of alkylating chemotherapeutic drugs on human testicular function have shown that in some cases virtually the only cell type present in patients' semen was round spermatids (12). Whether this phenomenon was due to general drug interference with induced damage to specific genes responsible for development beyond the round spermatid stage is not known; however, an occurrence of round-headed spermatozoa in two human brothers (29) suggests that morphology defects have a genetic origin.

Previous observations (8) have generally indicated that normally shaped mammalian sperm nuclei usually fluoresce green when stained with AO but often fluoresce red if the nucleus is misshaped. Recent studies by Evenson et al. (6,11) have shown a correlation between abnormal sperm head morphology and an increased sensitivity to denaturation of nuclear DNA in situ, i.e., fluorescing red after AO staining. This observation may be related to that of Gledhill et al. (18), who noted that misshapen sperm nuclei from subfertile bulls incorporated a higher level of $^3$H-Actinomycin D than normally shaped neighboring nuclei. Thus, it seemed reasonable to hypothesize that chemically induced abnormally shaped sperm would tend to fluoresce red after staining with AO. The work reported here shows that ENU induces both an increased percentage of abnormally shaped sperm and an increase in the CV of $\alpha_t$ values of the same sperm population either stained by the two-step AO or subjected to thermal stress prior to AO staining. Although the red fluorescing sperm were not sorted to determine the correlation between abnormal shapes and color of fluorescence, general observations of the stained samples under a fluorescence microscope indicated a high percentage of the abnormally shaped nuclei were red while normally shaped nuclei were green; some normally shaped nuclei were red. Further evaluation with the fluorescent microscope is difficult, since fading of fluorescence and adsorption of the AO to the glass slide make scoring inaccurate.

Figure 10 also shows a dose-dependent increase in a population of cells with a lower green fluorescence. Since this population was not seen in samples of isolated nuclei (Figure 12), it is a possible artifact induced by changes in whole sperm morphology. Future work will sort out this population and characterize it.

The difference in sperm chromatin structure that shifts the AO fluorescence from green to red is most likely related to an increased sensitivity for double-stranded DNA to denature to single-stranded DNA under the thermal stress and staining conditions. The nature of the chemically induced changes that produce this sensitivity is not understood. However, it should be noted in the two-step AO staining of epididymal whole sperm (Fig. 10), isolated nuclei (Table 1), or heated isolated nuclei (data derived from Fig. 12) that the total fluores-

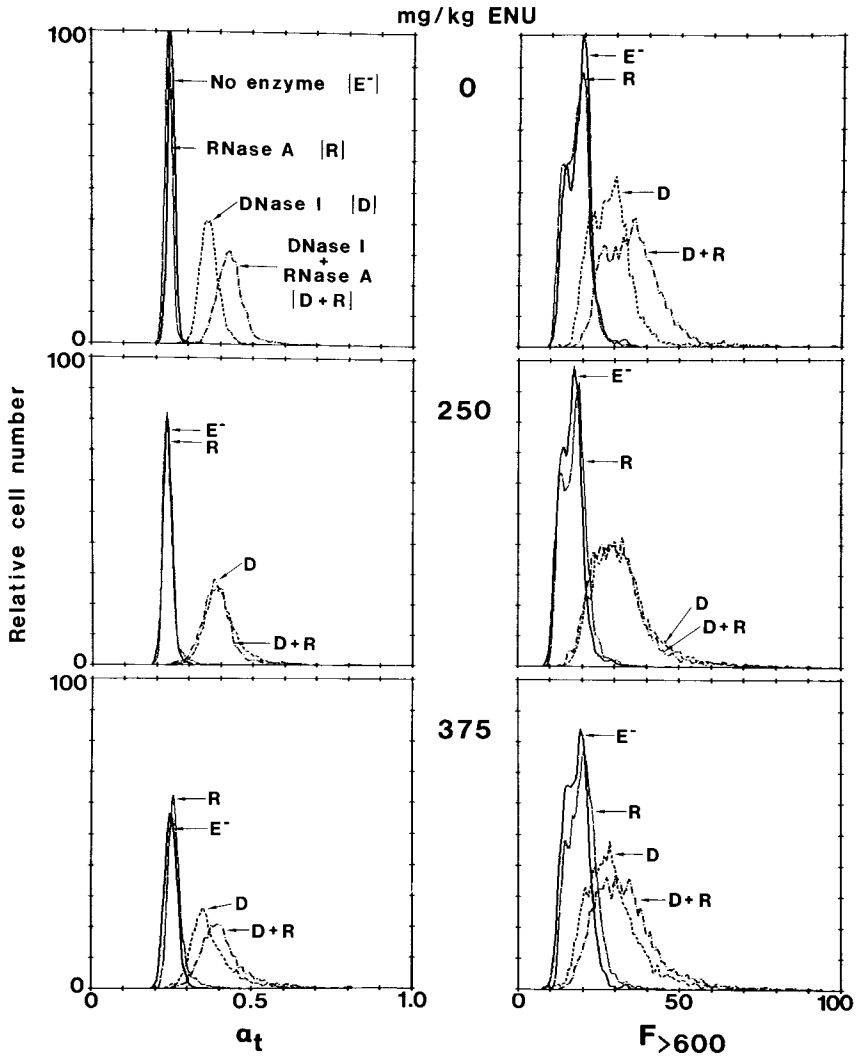


FIG. 15. Effect of DNAse I and/or RNAse digestion on red and green fluorescence of two-step AO stained fresh epididymal sperm nuclei obtained from mice treated with 0, 250, or 375 mg/kg ENU. The left and right hand columns display computer generated (plot program courtesy of Dr. Peter Rabinovitch) frequency histograms of $\alpha_t$ and red fluorescence values respectively. The values correspond to those in Table 1.

cence of sperm did not increase with increasing dose. Therefore, additional sites for DNA staining apparently do not become available in response to ENU treatment. These sites are potentially available, however, since mouse sperm treated with a disulfide reducing agent and protease will bind up to five times more AO than untreated sperm (9). Thus, it seems likely that the abnormally shaped sperm have the same protein constituents and level of disulfide bonding and that the primary difference is a higher proportion of DNA susceptible to interaction with AO and resulting in an increased ratio of red fluorescence. It is of interest that the shape of the curve for the CV of $\alpha_t$ derived from the two-step AO staining procedure is similar to that derived from the thermally denatured samples. The first step of the two-step AO procedures is a 30-sec treatment with a buffer containing 0.08 N HCl and 0.1% Triton X-100, which would also tend to partially denature the DNA.

Obviously, a key question is the nature of the chemically induced shift to red fluorescence. Among possibilities to consider are:

1. ENU interference with RNA metabolism, including alkylation of RNA, so that AO is staining abnormally residual RNA. This is an important consideration since in other studies (unpublished) we have observed in whole sperm cells that abnormal retention of red fluorescing material can be removed by sonication and/or RNAse treatment. The increased red fluorescence observed here is not due to this phenomena, however, since sonication and/or RNAse digestion did not reduce the level of red fluorescence in whole sperm, fresh or fixed nuclei. Furthermore, if significant amounts of RNA were present,

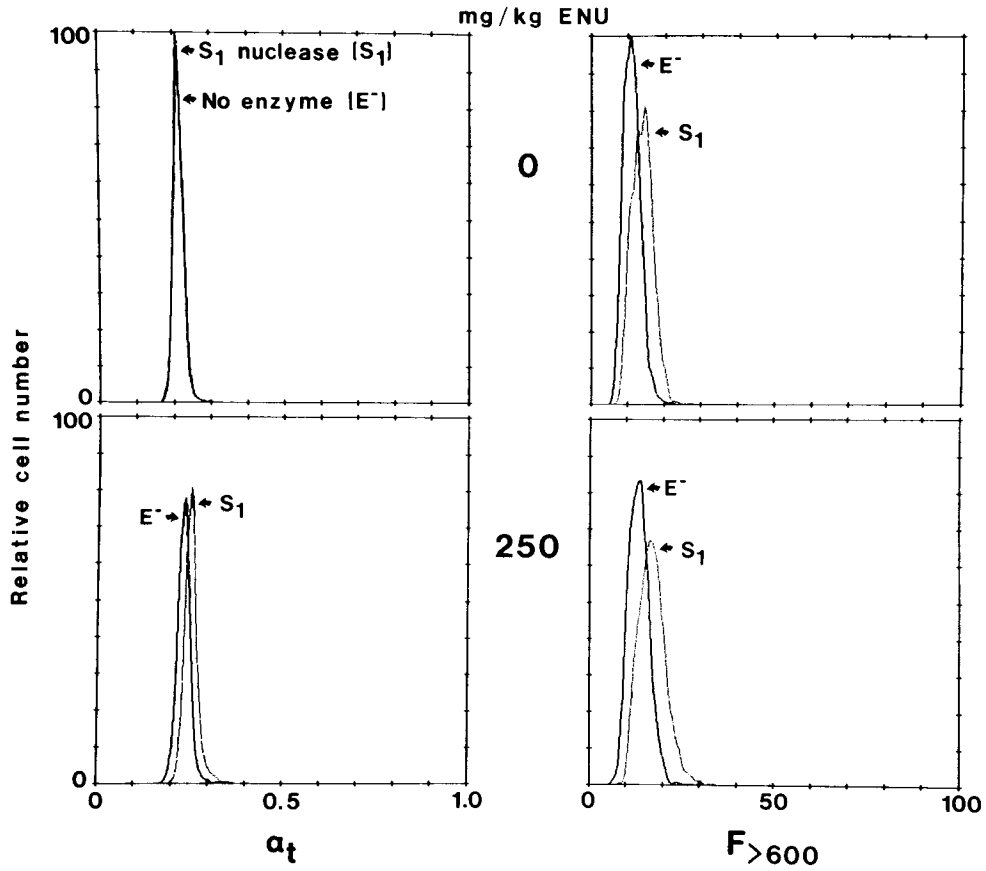


FIG. 16. Computer generated frequency histograms of $\alpha_t$ and red fluorescence values of fixed epididymal sperm nuclei obtained from mice exposed to either 0 or 250 mg/kg ENU, and then subjected to heat denaturation. Following heat denaturation, the nuclei were incubated for 2 h with nuclease $S_1$ prior to staining with AO and measuring by FCM.

the total fluorescence would have increased with dosage, which was not observed. Also note in Figure 3 that no testicular cell population obtained from ENU-treated mice had higher green or red fluorescence values than those from the control, indicating that DNA and RNA content was not increased in testicular cells. In agreement, light- and electron-microscopy studies of epididymal sperm showed no increase in cytoplasmic droplets and no evidence of nucleolar-like bodies.

Caution must be exercised in interpretation of enzyme digestion studies on sperm nuclei, since mature sperm chromatin is condensed to a level that permits only 20% of the available DNA sites to be stained with AO relative to AO stained round spermatids (9). Although a number of factors relate to the accessibility of various molecules to intranuclear sites, considering the small size of AO (MW = 302), larger molecules such as RNAse (MW = 13,700), nuclease $S_1$ (MW = 32,000–36,000) and DNAse I (MW = 31,000) may be excluded to a much greater extent.

2. ENU-induced breaks in DNA. ENU is a potent alkylating chemical that results in germ cell DNA strand breaks (37). However, since exposure to ENU was 28 days prior to measurements, it seems likely that repair would have been completed by this time; for example, most MMS-induced DNA strand breaks in mouse testicular cells are apparently repaired by 72 h (30). Conversely, repair of DNA strand breaks has in some cases been shown to take weeks (15). If some residual breaks remained in ENU-treated cells, heat- or acid-induced partial denaturation of DNA in situ would likely be increased and result in increased red fluorescence after AO staining. In this regard, it is of interest that DNAse I digestion dramatically increases nuclear red fluorescence, most likely due to AO interaction with newly exposed single-stranded segments. Conversely, clinical studies (6,7,12,14) argue against single-stranded DNA breaks as the only reason for increased red fluorescence, because a number of observations on patient sperm chromatin showed a high level of denaturation when there was no compelling reason to hypothesize that sperm DNA contained single-stranded breaks.

3. AO interaction with depurinated DNA. Alkylated regions of DNA are recognized by a complex enzyme system that excises the modified base from the DNA strand, degrades it, and resynthesizes the damaged section to reconstitute the complementary DNA strands (30). One might speculate that if the repair process were

not completed prior to nuclear condensation, depurinated regions might exist that could hypotheticaly interact with AO to produce red fluorescence. However, no evidence exists to indicate ENU-altered sperm DNA remains depurinated 28 days after alkylation.

4. Abnormal chromatin composition and/or condensation. DNA in somatic cells and early stages of spermiogenesis denatures at lower temperatures and to a much greater extent than in mature sperm (17,23). Thus, if disease or chemical exposure caused a lack of transition of histones for sperm-specific protamines this should interfere with condensation and lead to an increased susceptibility to denaturation, i.e., red fluorescence. Such a defect should also result in increased green (up to fivefold) and total fluorescence, which has been observed in human clinical samples (6), but was not observed here.

Through a number of detailed studies, the structure of mammalian sperm chromatin is becoming better understood; however, it is still difficult to speculate on possible alterations that result in increased red fluorescence after AO staining. Some studies on mammalian sperm chromatin suggest a nucleosome-like model (4), while other more convincing evidence favors a non-beaded, relatively smooth chromatin fiber that is formed during the histone to protamine transition in spermatids (27,1). Using x-ray studies, Wilkins (41) demonstrated that sperm nuclei were essentially crystalline aggregates of nucleoprotein. A recent and elegant study by Balhorn (1) suggests protamine is restricted to the minor groove of DNA, and neutralization of the phosphodiester backbone causes a compaction of the nucleochromatin structure.

On a speculative note, it is possible that the DNA in the condensed crystalline form may require "flexible joints," perhaps consisting of pyrimidine clusters along the DNA in order to accomodate the right packing. Inference for such flexible joints can be drawn from work on bacteriophage $T_4$ (20), salmon sperm (16), and hamster cells (13). Perhaps such hypothetical flexible joints do not become appropriately packaged as a result of abnormal spermiogenesis in response to chemicals, disease, or other factors, and these sites may be more susceptible to denaturation and interaction with AO. Also, DNA alkylation forming triesters with the phosphates of the DNA backbone (21) may, if not removed, possibly interfere with appropriate DNA-protein interactions necessary for normal chromatin condensation.

Although nuclease $S_1$ did not decrease red fluorescence (Fig. 16), we favor the view that some DNA was partially denatured but that it was renatured prior to AO staining and/or nuclease $S_1$ cannot effectively penetrate the highly condensed chromatin of fixed nuclei. In a somewhat similar type of experiment, but using different methods, Hunter et al. (23) favored the view that heat treatment of testicular sperm produces very little single-stranded DNA for enzymatic removal rather than the potentially denatured DNA is inaccessible to nuclease $S_1$.

The increased red fluorescence in acid- or heat-treated sperm cells obtained from ENU-exposed mice is apparently not due to residual RNA. Thus, we conclude from the data available at this time that the increased nuclear red fluorescence is due to DNA being more susceptible to partial denaturation in situ because of residual DNA damage or chromatin packing alterations.

Even though a number of parameters related to chemically induced sperm nuclear abnormalities are not understood, it is clear from these data that flow cytometry provides a very rapid means to assess damage to germ cell chromatin induced by toxic chemicals. These phenomena are not limited to ENU but occur in response to other mutagens, e.g., benzo(a)pyrene, ethyl and methyl methanesulfonate, and do not occur with other chemicals, e.g., caffeine (11 and unpublished data). Furthermore, these data demonstrate that two-parameter analysis (DNA, RNA) of testis samples provides a very rapid means to assess the ratio of cell types present following chemically induced cell kill and/or kinetic alterations of spermiogenesis.

## ACKNOWLEDGMENT

We thank Drs. M. Melamed and Z. Darzynkiewicz for their interest and valuable discussions.

We also thank Lorna Jost, Russell Gesch, Rebecca Baer, and Jisoo Lee for technical assistance and Elsa Wood for help in preparing this manuscript.

## LITERATURE CITED

1. Balhorn R: A model for the structure of chromatin in mammalian sperm. J Cell Biol 93:298–305, 1982.
2. Beatty RA: The genetics of the mammalian gamete. Biol Rev 45:73–119. 1972.
3. Bradley DF, Wolf MK: Aggregation of dyes bound to polyanions. Proc Natl Acad Sci USA 45:944–952, 1959.
4. Chevaillier P: Some aspects of chromatin organization in sperm nuclei. In: The Sperm Cell, Andre, J (ed). Martinus Nijhoff Publishers, The Hague, 1983, pp 179–196.
5. Darzynkiewicz Z, Traganos F, Sharpless T, Melamed MR: Lymphocyte stimulation: A rapid multiparameter analysis. Proc Natl Acad Sci USA. 73:2881–2884, 1976.
6. Evenson, DP: Male germ cell analysis by flow cytometry: Effects of cancer, chemotherapy and other factors on testicular function and sperm chromatin structure. In: Clinical Cytometry, Andreef, MA (ed) NY Acad Sci, New York, 1985.
7. Evenson DP, Arlin A, Welt S, Claps ML, Melamed MR: Male reproductive capacity may recover following drug treatment with the L-10 protocol for acute lymphocytic leukemia (ALL). Cancer 53:30–36, 1984.
8. Evenson DP, Darzynkiewicz Z, Melamed MR: Relation of mammalian sperm chromatin heterogeneity to fertility. Science 210:1131–1133, 1980.
9. Evenson DP, Darzynkiewicz Z, Melamed MR: Comparison of human and mouse sperm chromatin structure by flow cytometry. Chromosoma 78:225–238, 1980.
10. Evenson DP, Higgins PJ, Melamed MR: Detection of male reproductive abnormalities by FCM measurement of testicular and ejaculated germ cells. In: Biological Dosimetry: Cytometric Approaches to Mammalian Systems, Eisert WG, Mendelsohn ML, (eds). Springer-Verlag, New York, 1984, pp 99–110.
11. Evenson DP, Jost L, Gesch R, Ballachey B: Effect of ethyl methanesulfonate on mouse testicular function. In Proceedings of Analytical Cytology X, June 3–8 1984, Asilomar Conference Grounds, Pacific Grove, CA. Abstract A49, 1984.

12. Evenson DP, Klein FA, Whitmore WF, Melamed MR: Flow cytometric evaluation of sperm from patients with testicular carcinoma. J Urol 132:1220–1225, 1984.
13. Evenson DP, Mego WA, Taylor JH: Subunits of chromosomal DNA. I. Electron microscopic analysis of partially denatured DNA. Chromosoma 39:225–235, 1972.
14. Evenson DP, Melamed MR: Rapid analysis of normal and abnormal cell types in human semen and testis biopsies by flow cytometry. J Histochem Cytochem 31:248–253, 1983.
15. Farber E: On the pathogenesis of experimental hepatocellular carcinoma. In: Hepatocellular Carcinoma, Okuda K, Peters RL (eds). J. Wiley & Sons, Inc., New York, 1976, pp 3–22.
16. Giannoni G, Padden FJ Jr, Keith, HD: Crystallization of DNA from dilute solutions. Proc Natl Acad Sci USA 62:964-971, 1969.
17. Gledhill BL, Campbell GL: Microfluorimetric comparison of chromatin during cytodifferentiation. In: Fluorescence Techniques in Cell Biology, Thaer AA, Sernetz M (eds). Springer-Verlag, New York, 1973, pp 151–162.
18. Gledhill BL, Darzynkiewicz Z, Ringertz J: Changes in deoxyribonucleoprotein during spermiogenesis in the bull: Increased [$^3$H] Actinomycin D binding to nuclear chromatin of morphologically abnormal spermatozoa. J Reprod Fertil 26:25–38, 1971.
19. Gledhill BL, Lake S, Steinmetz LL, Gray JW, Crawford JR, Dean PN, Van Dilla MA: Flow microfluorometric analysis of sperm DNA content: Effect of cell shape on the fluorescence distribution. J Cell Physiol 87:367–376, 1976.
20. Gray HB Jr, Hearst JE: Flexibility of native DNA from the sedimentation behavior as a function of molecular weight and temperature. J Mol Biol 35:111–129, 1968.
21. Hodgson, E, Guthrie FE: Introduction to biochemical toxicology. Elsevier, New York, 1980, pp 310–329.
22. Hugenholtz, AP, Bruce WR: Transmission of radiation-induced elevations in abnormally shaped murine sperm. Proc 8th Ann Meet Environ Mutagen Soc, 1977.
23. Hunter JD, Bodner AJ, Hatch FT, Balhorn RI, Mazorimas JA, McQueen AP, Gledhill BL: Single-strand nuclease action on heat-denatured spermiogenic chromatin. J Histochem Cytochem 24:901–907, 1976.
24. IARC Working Group on the Evaluation of the Carcinogenic Risk ot Chemicals to Humans. N-nitroso-N-ethylurea. International Agency for Research on Cancer Monograph 17:191–215, 1978.
25. Kapuscinski J, Darzynkiewicz Z: Denaturation of nucleic acids induced by intercalating agents. Biochemical and biophysical properties of acridine orange-DNA complexes. J Biomolecular Struct Dynamics 1:1485–1499, 1984.
26. Kapuscinski J, Darzynkiewicz Z, Melamed MR: Luminescence of the solid complexes of acridine orange with RNA. Cytometry 2:201–211, 1982.
27. Kierszenbaum AL, Tres LL: The packaging unit: A basic structural feature for the condensation of late cricket spermatid nuclei. J Cell Sci 33:265–283, 1978.
28. Krzanowska H: Inheritance of sperm head abnormality types in mice: The role of the Y chromosome. Genet Res 28:189–198, 1976.
29. Kullander S, Rausing A: On round-headed spermatozoa. Int J Fertil 20:33–40, 1975.
30. Lee IP: Adaptive biochemical repair response toward germ cell DNA damage. Am J Indust Med 4:135–147, 1983.
31. Lerman LS: The structure of the DNA-acridine complex. Proc Natl Acad Sci USA 49:94–102, 1963.
32. Lewis SE, Johnson FM, Skow LC, Barnett LB, Popp RA: Mosaic mutations among the progeny of parents treated with ethylnitrosourea (abstract). Environ Mut Soc 15:72, 1984.
33. Meistrich ML, Lake S, Steinmetz LG, Gledhill BL: Flow cytometry of DNA in mouse sperm and testis nuclei. Mut Res 49:383–396, 1978.
34. Rodriguez M, Panda BB, Ficsor G; Testes weight reflect ethylnitrosourea induced histopathology in mice. Toxicol Lett 17:77–80, 1983.
35. Russell WL, Hunsicker PR: Mutagenic effect of ethylnitrosourea (ENU) on post-stemcell stages in male mice (abstract). Environ Mut Soc 15:71, 1984.
36. Russell WL, Kelly EM, Hunsicker PR, Bangham JW, Maddox SC and Phipps EL: Specific locus test shows ethylnitrosourea to be the most potent mutagen in the mouse. Proc Natl Acad Sci USA 76:5815–5819, 1979.
37. Skare JA, Schrotel KR, Detection of strand breaks in rat germ cell DNA by alkaline elution and criteria for the determination of a positive response (abstract). Environ Mut Soc 15:130, 1984.
38. Staub JE, Matter BE: Heritable reciprocal translocations and sperm abnormalities in the $F_1$ offspring of male mice treated with triethylene melamine (TEM). Archiv fur Genetik 49:29–41, 1976.
39. Topham JC: The Detection of carcinogen-induced sperm head abnormalities in mice. Mutat Res 69:149–155, 1980.
40. Topham JC: Chemically-induced transmissible abnormalities in sperm head shape. Mutat Res 70:109–114, 1980.
41. Wilkins MHF: Physical studies of the molecular structure of deoxyribose nucleic acid and nucleoprotein. Cold Spring Harbor Symp Quant Biol 21:75–90, 1956.
42. Wyrobek AJ: Changes in mammalian sperm morphology after x-ray and chemical exposure. Genetics 92:105–119, 1979.
43. Wyrobek AJ, Bruce WR: Chemical induction of sperm abnormalities in mice. Proc Natl Acad Sci USA 72:4425–4429, 1975.
44. Wyrobek AJ, Bruce WR: The induction of sperm shape abnormalities in mice and humans. In: Chemical Mutagens: Principles and Methods for Their Detection, Vol 5, Hollaender A, DeSerres FJ (eds). Plenum press, New York, 1978, pp 257–285.
45. Wyrobek AJ, Gordon LA, Burkhart JG, Francis MW, Kapp Jr. RW, Letz G, Malling HV, Topham JC, Whorton MD: An evaluation of the mouse sperm morphology test and other sperm tests in nonhuman mammals: A report of the US Environmental Protection Agency Gene-tox Program. Mutat Res 115:1-72, 1983.